

Tolerance in Thalamic Paraventricular Nucleus Neurons Following Chronic Treatment of Animals with Morphine

Omar Koita, Joseph J. Lebowitz, and  John T. Williams

Vollum Institute, Oregon Health & Science University, Portland, Oregon 97239

Abstract

Neurons in the paraventricular nucleus of the thalamus (PVT) integrate visceral and limbic inputs and project to multiple brain regions to bias behavior toward aversive or defensive states. This study examines MOR signaling in anterior PVT neurons in brain slices from untreated and morphine-treated animals. Imaging in a MOR-Cre reporter rat revealed extensive expression in aPVT cells, and the application of [Met]⁵⁻ enkephalin (ME) induced outward currents which were abolished by the MOR-selective antagonist CTAP. A saturating concentration of ME resulted in desensitization that was blocked by compound 101, indicating a phosphorylation-dependent process. The opioid sensitivity of amygdala-, nucleus accumbens-, and prefrontal cortex-projecting neurons was then examined. Neurons that projected to the amygdala were more sensitive to ME than cortical- and accumbal-projecting cells. Following chronic treatment, tolerance to morphine was found in neurons projecting to the amygdala and nucleus accumbens with a trend toward tolerance observed in neurons projecting to the prefrontal cortex. The results reveal that adaptations to chronic opioid exposure are in the aPVT circuits contribute to affective pain processing and may provide specific insights into the etiology of withdrawal following the cessation of opioid use.

Key words: desensitization; morphine; neuronal excitability; opioids; tolerance; withdrawal

Significance Statement

The PVT connects visceral sensation to cognitive and limbic nuclei with a particularly strong role in pain processing. Nearly all neurons in the anterior PVT (aPVT) neurons express opioid receptors, suggesting that this brain region likely contributes to affective and cognitive facets of opioid analgesia and dependence. Understanding the acute actions and adaptations induced by opioids in the PVT therefore provide insight into affective pain processing and potentially connect it to the affective withdrawal symptoms seen in opioid use disorder.

Introduction

The analgesic tolerance seen following sustained opioid exposure is mediated by adaptive processes that counter the continued activation of opioid receptors on both rapid and extended timescales. These include receptor-dependent tolerance, marked by a decrease in the coupling of receptors to effectors that reduces signaling efficacy. Phosphorylation of μ -opioid receptors (MORs), which leads to the recruitment of β -arrestin and triggers receptor desensitization and internalization, is critical for receptor-dependent tolerance (Williams et al., 2013). However, receptor-dependent tolerance is cell type specific, with a range of adaptations observed across distinct brain regions (Levitt and Williams, 2018; Birdsong and Williams, 2020). Adaptive processes beyond receptor tolerance include changes in neuronal excitability, synaptic plasticity, and circuit-level adaptations that oppose the continued presence of opioids. Upon termination of opioid exposure, these adaptive processes reverse more slowly than receptor inactivation, often revealing

Received June 9, 2024; revised April 21, 2025; accepted April 30, 2025.

The authors declare no competing financial interests.

Author contributions: O.K., J.J.L., and J.T.W. designed research; O.K. and J.J.L. performed research; O.K. and J.J.L. analyzed data; O.K., J.J.L., and J.T.W. wrote the paper.

This work was supported by the National Institutes of Health DA04523 (J.T.W.) and F99NS129176 (O.K.). We thank Marina Wolf for providing MOR-Cre × tdTomato rats for imaging experiments. We thank Seksiri Arttamangkul and Skyler Jackman for helpful comments on the analysis and presentation of this work.

Continued on next page.

hypertrophic signaling believed to contribute to symptoms of withdrawal. The causal contributions of withdrawal symptoms to opioid use disorder, particularly those that involve affective processing, remain under intense investigation (Koob, 2013; Koob and Volkow, 2016). Thus, understanding the acute and chronic actions of opioids in brain regions that participate in affective pain processing represent a critical locus in the understanding of opioid use disorder and the emergence of withdrawal symptoms.

The paraventricular nucleus of the thalamus (PVT) is a midline thalamic structure that integrates information from subcortical (i.e., limbic) and cortical (i.e., cognitive) nuclei (Li and Kirouac, 2012; Kirouac, 2015; Otis et al., 2019; Penzo and Gao, 2021). The PVT plays a crucial role in emotional and motivational aspects of behavior including arousal, stress, and reward processing, and it has been implicated in the actions of opioids and opioid dependence (Bengoetxea et al., 2020; Chisholm et al., 2020; Keyes et al., 2020; Giannotti et al., 2021; Yu et al., 2021; Babaei et al., 2023; Zhu et al., 2023; McDevitt et al., 2024; Panaccia et al., 2024). PVT signaling contributes to changes in arousal (Gao et al., 2020; Bu et al., 2022; Zhao et al., 2022; Eacret et al., 2023; Duan et al., 2024) and pain awareness (Chang et al., 2019; Zhang et al., 2022, 2023) associated with opioid withdrawal, signifying specific contributions to the widely distributed phenomenon. Previous studies have shown that both spontaneous and antagonist-induced withdrawal increase *c-fos* expression in PVT neurons (Chahl et al., 1996; Zhu et al., 2016), suggesting heightened neuronal activity during withdrawal. The PVT projections to brain regions that regulate affective state implicate this increased activity in emotional components of withdrawal that drive continued or renewed drug seeking. However, the acute actions of MORs and the adaptive processes caused by chronic opioid exposure in PVT cells that project to these brain regions remain to be characterized.

The PVT is a heterogeneous population of neurons commonly divided into the anterior (aPVT) and posterior PVT (pPVT; Li and Kirouac, 2012; Gao et al., 2020; Rivera-Irizarry et al., 2023; Shima et al., 2023). Firing properties (Kolaj et al., 2012, 2014; McDevitt and Graziane, 2019), and gene expression profiles (Gao et al., 2020) further distinguish PVT neurons. Despite this heterogeneity, there is a uniformly dense expression of opioid receptors (Eacret et al., 2023; Hou et al., 2023). The aPVT in particular sends strong projections to limbic circuits implicated in opioid tolerance and withdrawal, including the nucleus accumbens and amygdala, and has been shown to have higher MOR expression relative to other thalamic regions (Chang et al., 2019; Hou et al., 2023). The PVT projection to the nucleus accumbens (NAc) has been specifically examined with respect to opioid use disorder as projections from the PVT to the NAc mediate active avoidance and gate the expression of opioid withdrawal behaviors (Zhu et al., 2016; Dong et al., 2020; Ma et al., 2021; Kanai et al., 2022; McDevitt et al., 2024). Other key projections from the PVT include the amygdala (AM) and medial prefrontal cortex (mPFC; Li and Kirouac, 2008; Gao et al., 2020), which contribute to the incubation of drug craving (Pickens et al., 2011). The projection from aPVT to amygdala encodes emotional valence (Barson et al., 2020; Kirouac, 2015; O'Neill et al., 2023; Penzo et al., 2015; Piantadosi et al., 2024), and projections to the basolateral amygdala (BLA) have been shown to modulate neuropathic pain and emotional anxiety (Tang et al., 2024). The mPFC is known to play a role in the preoccupation phase of opioid addiction (Koob and Volkow, 2016), and increased activity in the projections from the PVT to the mPFC have been shown to increase arousal and fear memory retrieval (Huong et al., 2006; Padilla-Coreano et al., 2012).

Despite the recognized importance of these projection-defined circuits, the acute activation of MORs and the adaptive processes resulting from chronic morphine treatment in projection-defined neurons of the PVT have not been fully characterized. Understanding the projection-specific acute and chronic actions of opioids is critical for elucidating the neural mechanisms underlying distinct components of opioid tolerance and withdrawal.

The present investigation examines the acute and chronic activation of MORs on aPVT neurons and the heterogeneity of these effects on cells that project to the NAc, amygdala, or mPFC. Acutely, aPVT neurons projecting to the amygdala were more sensitive than neurons projecting to the NAc and mPFC. Following chronic morphine treatment, neurons that projected to the amygdala and NAc developed increased receptor-dependent tolerance to morphine. The results indicate that chronic morphine treatment results in cellular adaptations in the neurons that project to three brain areas critically implicated in opioid use disorder.

Correspondence should be addressed to John T. Williams at williamj@ohsu.edu.

Copyright © 2025 Koita et al.
This is an open-access article distributed under the terms of the [Creative Commons Attribution 4.0 International license](https://creativecommons.org/licenses/by/4.0/), which permits unrestricted use, distribution and reproduction in any medium provided that the original work is properly attributed.

Materials and Methods

Drugs. Morphine sulfate was obtained from the National Institute on Drug Abuse, Neuroscience Center. [Met⁵]-enkephalin (ME), bestatin, and thiorphan were acquired from Sigma-Aldrich. (RS)-Baclofen was purchased from Tocris. Stock solutions of ME and baclofen were dissolved in water, diluted to the appropriate concentration in artificial cerebrospinal fluid (ACSF), and applied by superfusion.

Animals. Rats of both sexes between 5 and 8 weeks old were used for all experiments. Wild-type Sprague Dawley rats were obtained from Charles River Laboratories and maintained using approved breeding and husbandry procedures. MOR-cre rats were obtained from NIH (Bossert et al., 2023) and crossed with a floxed-tdTomato reporter rat (Igarashi et al., 2016), and offspring positive for both transgenes were provided by Dr M. Wolf at OHSU. All protocols and experiments were conducted in accordance with National Institutes of Health guidelines and with approval from the Institutional Animal Care and Use Committee of Oregon Health & Science University.

Viral injections. Animals [postnatal day (P) 23–26] were anesthetized with 4% isoflurane and placed in a stereotaxic frame. Anesthesia was maintained with isoflurane (2.5%) and confirmed periodically by a lack of toe pinch response for microinjection of viral vectors. Injections of a retrograde adeno-associated virus (AAV) encoding green fluorescent protein (AAVrg-CAG-GFP) was carried out with the following coordinates (from bregma). (1) The amygdala (AM, anteroposterior: –2.5 mm, mediolateral: ±3 mm, dorsoventral: –6.95 mm). (2) The nucleus accumbens (NAc) anteroposterior: +1.7 mm, mediolateral: ±0.7 mm, dorsoventral: –7 mm. (3) Medial prefrontal cortex (mPFC anteroposterior: +1.8 mm, mediolateral: ±0.5 mm, dorsoventral: –4.25 mm). A total of 200 nl of each virus was injected at 1 nl/s bilaterally in all regions. Electrophysiology experiments were carried out at least 2 weeks after injection.

Chronic opioid treatment. Rats were treated with morphine sulfate continuously released from osmotic pumps as described previously (Quillinan et al., 2011). Osmotic pumps (2 ML1; Alzet) were filled with the required concentration of morphine (in water) to deliver 80 mg/kg/d at 10 µl/h for up to 7 d. The dose was chosen to induce the maximum amount of tolerance over the relatively short duration of application. For pump implantation, rats were anesthetized with 4% isoflurane, and anesthesia was maintained with 2.5% isoflurane. An incision was made in the midscapular region and osmotic pumps were implanted subcutaneously. The incision was then closed with 4–5 stainless steel wound closure clips (Stoelting; #59027), and animals were monitored to ensure stable healing. Pumps remained until animals were used for experiments 6 or 7 d later.

Ex vivo slice preparation. Rats were deeply anesthetized using isoflurane and killed by cardiac percussion. Brains were excised, trimmed, and mounted adjacent to a 3% agar block (caudal edge) for slicing with a vibratome (VT 1200S; Leica). Horizontal PVT slices (272 µm) were prepared in warmed (~34°C) and oxygenated (95% O₂/5% CO₂) ACSF containing the following (in mM): 126 NaCl, 2.5 KCl, 1.2 MgCl₂, 2.4 CaCl₂, 1.2 NaH₂PO₄, 21.4 NaHCO₃, 11.1 D-glucose, and 10 µM MK-801 (to prevent NMDA-mediated excitotoxicity). Slices were allowed to recover in oxygenated ACSF at 34°C containing 10 µM MK-801 for ≥30 min and stored in oxygenated ACSF at 34°C until use. In experiments to assess tolerance and withdrawal, protocols were identical to those above with the addition of morphine hydrochloride (1 µM) to ACSF during extraction, slicing, recovery, and experiments.

Electrophysiology. Slices were transferred to the recording chamber and continuously superfused with ACSF (1.5–2 ml/min, at 34°C). Recording pipettes (World Precision Instruments) with a resistance of 2–3 MΩ were filled with an internal solution containing the following (in mM): 100 potassium methanesulfonate, 20 NaCl, 1.5 MgCl₂, 5 HEPES(K), 2 BAPTA (4K), 2 Mg-ATP, 0.3 NaGTP, adjusted to pH 7.35, and 275–280 mOsm. Whole-cell recordings from aPVT neurons were obtained using an Axopatch 1D amplifier (Axon Instruments) in voltage-clamp mode ($V_{\text{hold}} = -70$ mV). Data was collected at 20 kHz and filtered at 10 kHz using AxoGraph X, and recordings were continuously monitored using PowerLab (Chart version 5.4.2; ADInstruments). Membrane resistance, capacitance, and series resistance were determined using the average of 20 5 mV pulses following break-in and were continuously monitored and checked upon termination of recordings. Cells were excluded if the series resistance at break-in was >20 MΩ, and experiments were terminated if the series resistance increased by >20% during recordings. Opioid currents were determined by the difference in the initial holding current and that induced by opioid agonists. Experiments that determined the current induced by morphine after chronic exposure were determined by the inward current induced by naloxone in the continued presence of morphine.

Quantification of MOR-positive neurons. Rats expressing iCre recombinase under control of the endogenous *Oprm1* promoter were crossed with a floxed-tdTomato reporter rat to generate rats with tdTomato expression restricted to MOR-expressing cells (Bossert et al., 2023; Igarashi et al., 2016). Slices for immunolabeling were generated using identical procedures as those for electrophysiology experiments. Following recovery, slices were fixed in 4% PFA in PBS for 1 h at room temperature. Fixed slices were blocked and permeabilized using PBS containing 0.5% Triton X-100 and 10% normal goat serum for 1 h at room temperature. Immunolabeling of NeuN (Millipore MAB377, 1:500) was conducted overnight at 4°C in PBS containing 0.1% Triton X-100 and 5% normal goat serum. Slices were washed three times for 20 min each in PBS at room temperature before secondary labeling with Goat anti-Mouse Alexa Fluor Plus 647 (Invitrogen A32728, 1:500)

for 1 h at room temperature. Slices were then washed in PBS five times for ≥ 30 min each before being mounted on slides using Fluoromount-G (SouthernBiotech). Slides were cured overnight at room temperature and imaged the following day.

Imaging was conducted on a Zeiss LSM 710 controlled by Zeiss Zen software. An initial 10 \times image was taken to locate and define the aPVT using its position relative to the third ventricle. For quantification, tdTomato and NeuN signals were acquired sequentially to create Z-stacks ($425 \mu\text{m} \times 425 \mu\text{m} \times 10 \mu\text{m}$ in $x/y/z$) using a 20 \times objective and large (~ 2.5 AU) pinhole with identical laser and detection settings for all images. Images were denoised using Zen and maximum-intensity-projections were generated and tdTomato- and NeuN-positive cells were manually identified using individual channel images and the annotation function in Zen. Cells were then classified as positive for both NeuN and tdTomato using the independent designations and confirmed to be the same cell by shared morphology. The image presented is a representative maximum intensity projection used for quantification.

Two-photon imaging. Two-photon imaging of cells expressing the AAV_{retro}-GFP construct was carried out on a custom-built microscope using an Olympus BX51W1 upright platform and an Olympus 60 \times /1.0 NA water immersion LUMFI objective. Excitation was achieved using a Chameleon Ti:sapphire tunable laser at 910 nm. Image acquisition was conducted using ScanImage software (Pologruto et al., 2003). Z-stacks containing representative GFP-positive cells were generated at 2 μm steps and maximum intensity projections are shown.

Data analysis. Sample sizes were not predetermined. For all experiments, 2–5 animals were used to obtain at least five technical replicates (cells) per group. Analysis was performed in AxoGraph X and statistics in GraphPad Prism 9. Values are presented as mean \pm SEM or mean \pm 95% confidence intervals as indicated in figure legends. Statistical comparisons were made using unpaired t test, Kruskal–Wallis, one-way or two-way ANOVA, as well as multiple comparison-adjusted Tukey's post hoc tests, Dunnett T3, and Šidák's test, as appropriate. For all experiments, $p < 0.05$ was used to define statistical significance.

Results

Opioid receptors in the aPVT

There is a high density of neurons that express MOR in the PVT (Mansour et al., 1994; Arvidsson et al., 1995; Le Merrer et al., 2009). The percentage of aPVT neurons that express MOR was determined by quantifying the coexpression of tdTomato with expression restricted to *Oprm1* positive cells (see methods) and NeuN immunolabeling. The results show that the vast majority ($\sim 87\%$) of aPVT neurons coexpressed tdTomato and NeuN, though a small population of NeuN-positive cells that did not express tdTomato were observed ($n = 531$ cells/6 slices/2 animals; Fig. 1A). The MOR-mediated component of outward currents induced by ME was examined using whole-cell recording from the same *Oprm1*-Cre:tdTomato reporter animals (Extended Data Fig. 1-1). Application of ME (10 μM) induced an outward current (93.0 ± 8.9 pA, $n = 6$) that was blocked by coapplication of the MOR-selective antagonist, CTAP (1 μM ; 8.9 ± 3.9 pA, 5 cells from 3 animals; $p = 0.0003$, unpaired t test). In experiments with wild-type animals, the application of ME (10 μM) or the photoactivation of caged [Leu]⁵-enkephalin (CYLE; Banghart and Sabatini, 2012) induced outward currents that ranged from 20 to 240 pA (ME 10 μM 84.9 ± 11.3 pA, 21 cells from 9 animals; CYLE 94.9 ± 9.6 pA, 35 cells from 13 animals, $p = 0.5$ unpaired t test) in amplitude (Fig. 1B–D). Thus, the majority of aPVT neurons express MORs that induce an outward current when activated.

An outwardly rectifying potassium conductance

The conductance induced by MOR activation was examined by the construction of current/voltage plots. The currents induced by ramp potentials from -55 to -125 mV were measured before and following photoactivation of caged [Leu]⁵-enkephalin (CYLE; Fig. 2). A solution containing CYLE (50 μM) was perfused for a minimum of 5 min. Two 1 s ramp potentials from -55 to -125 mV were made 15 s apart in CYLE-containing ACSF. Before the second ramp, a 50 ms pulse of UV light (356 nm) was applied to photoactivate CYLE (Fig. 2A). Photoactivation resulted in an outward current measured at -55 mV in all cells tested (94.9 ± 9.6 pA, $n = 35$ cells from 13 animals; Fig. 1D). The current activated by CYLE during the potential ramp following photo activation was subtracted from the control ramp to obtain the CYLE-induced current (Fig. 2B,C). The opioid current induced by CYLE uncaging reversed at the potassium equilibrium potential (-97.8 mV, measured -95.5 ± 5.1 mV, $n = 6$ from 5 animals). Unexpectedly however, the opioid current measured at potentials more negative than the potassium equilibrium potential did not increase in amplitude as expected from an inwardly rectifying potassium conductance (G-protein-gated inwardly rectifying potassium conductance, GIRK). Similar results were found using voltage steps (10 mV) made from -45 to -125 mV with the current at each step measured in the absence and presence of ME (10 μM ; Extended Data Fig. 2-1).

To further characterize the CYLE-induced outward current, the reversal potential of the current was measured in separate experiments where the potassium concentration in the extracellular solution was changed from 2.5 mM to 6.5 and 10.5 mM (Fig. 2D). The reversal potential of the CYLE-induced current measured in each concentration of potassium was -95.5 ± 5.1 mV (in 2.5 mM), -74.8 ± 3.0 (in 6.5 mM), and -62.5 ± 4.1 mV (in 10.5 mM; $n = 6$ from 5 animals). The predicted potentials based on the Nernst equation for a potassium and the observed reversal potentials were plotted as a function of the extracellular potassium indicating that the opioid current aligns well with the activation of a potassium

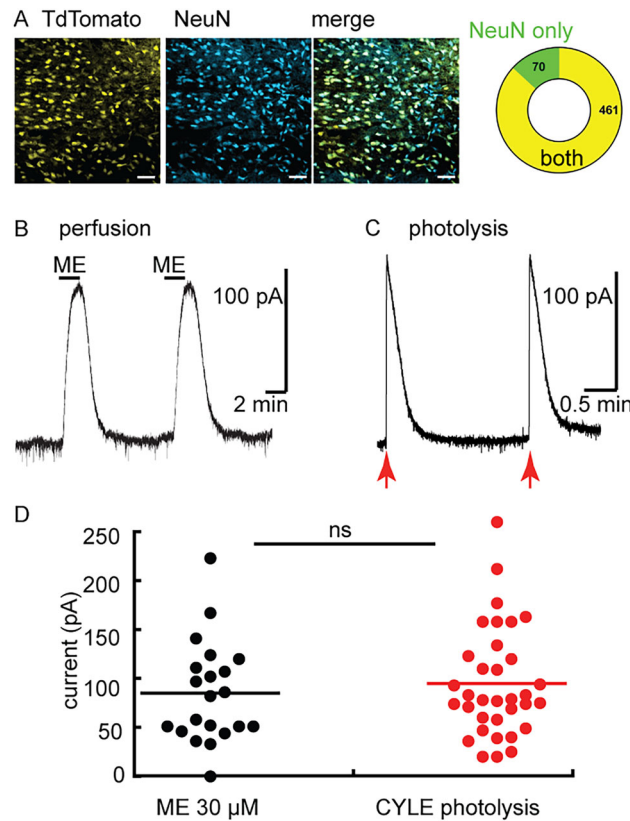


Figure 1. Dense expression of functional opioid receptors in the aPVT. **A**, Representative images of NeuN immunolabeling and tdTomato expression in rats conditionally expressing tdTomato in MOR-positive cells. Left, Cre-dependent tdTomato cells; middle, immunofluorescence for NeuN indicating all neurons; and right, merged image of the two channels. Scale bar, 50 μm . Far right, Quantification indicating the number of cells that expressed both tdTomato and NeuN and cells that were stained with NeuN but did not express the tdTomato reporter ($n = 531$ cells/6 slices/2 animals). **B**, Example recording showing the outward current induced by perfusion of ME (10 μM). **C**, Example recording showing the outward current induced by photoactivation of CYLE. Arrows indicate the timing of a UV flash (50 ms, 5 mW). **D**, Summarized results showing the outward current induced by perfusion of ME and photoactivation of CYLE (7 cells, 3 animals). The results indicate that activation of opioid receptors in the majority of neurons in the aPVT induced an outward current. Neurons in the aPVT express MORs. Supported by Extended Data Figure 1-1.

conductance (Fig. 2D). The application of BaCl_2 (1 mM) blocked the opioid current (Extended Data Fig. 2-2), further indicating an increase in potassium conductance. Because of the lack of inward rectification, it was not clear that the conductance was mediated by G-protein-gated inwardly rectifying potassium (GIRK) channels. The GIRK1 activator, ML297, was examined to determine if GIRK channels contributed to the conductance (Wydeven. et al., 2014). Application of ML297 (10 μM) did not affect the resting conductance but increased the outward opioid current suggesting that GIRK1 was involved (Extended Data Fig. 2-3). In the presence of ML297, the overall shape of the current/voltage plot did not change at potentials negative to the potassium equilibrium potential (Extended Data Fig. 2-3). The increase in the opioid current induced by ML297 between -55 and -115 mV was measured by subtracting the opioid-sensitive current obtained in control conditions from that in the presence of ML297 (Extended Data Fig. 2-3D). The result showed that the ML297-sensitive opioid current rectified outwardly similar to the current in control. Thus, this potassium conductance differed from the GPCR-dependent activation of GIRK observed in other neurons (Lüscher and Slesinger, 2010).

Acute desensitization is phosphorylation dependent

Acute desensitization induced by a saturating concentration of an efficacious agonist, such as ME, varies among different neurons. For example, ME-induced desensitization in the LC is considerably larger than in neurons of the Kölliker–Fuse (Levitt and Williams, 2018). In the present study application of a saturating concentration of ME (30 μM) resulted in a peak outward current that declined to $65.4 \pm 5.3\%$ of the peak in 10 min ($n = 15$ cells from 11 animals; Fig. 3C). Acute desensitization is known to be dependent on phosphorylation of the C terminus of MOR by G-protein kinase (GRK; Lowe et al., 2015; Leff et al., 2020). The role of GRK in desensitization in aPVT cells was examined in slices incubated in the GIRK2/3 blocker, compound 101 (30 μM , 1 h). The amplitude of the initial current induced by ME (30 μM) was not significantly different in the absence (88.9 ± 10.8 pA) versus presence (89.9 ± 11.3 pA) of compound 101 (Fig. 3B; $p = 0.4762$; control: $n = 15$ cells from 5 animals; CMP101: $n = 10$ cells from 7 animals). In the presence of compound 101, however, desensitization induced by ME was completely blocked (remaining current at 10 min: $91.35 \pm 0.03\%$; Fig. 3A,C). Thus, the desensitization of MORs in the aPVT is dependent on phosphorylation induced by GRK2/3.

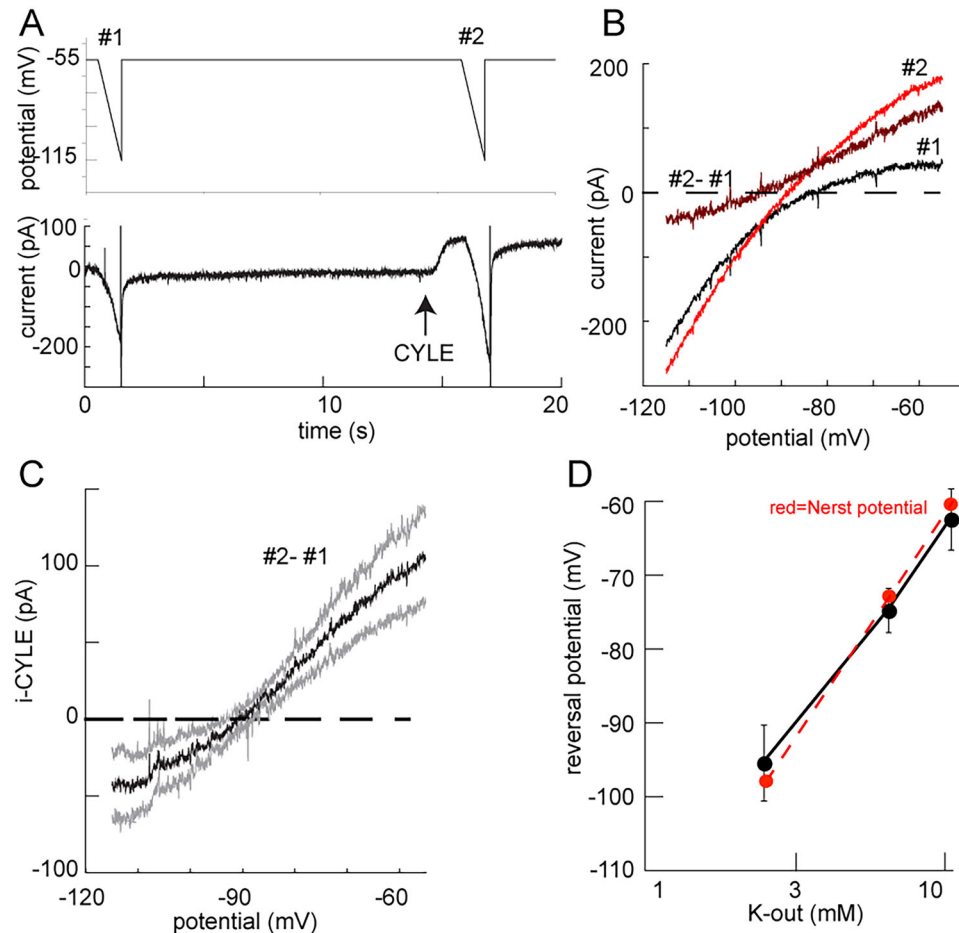


Figure 2. An outward rectifying potassium conductance is activated by opioid receptors. **A**, An illustration of the protocol used to obtain the current/voltage plots. Two voltage ramps were applied and the currents induced during the ramps were measured before (#1) and following (#2) the photoactivation of CYLE. **B**, Currents were recorded during voltage ramps. The current prior to photoactivation (#1) was subtracted from that following photoactivation of CYLE (#2) to obtain the isolated opioid-induced current. **C**, Summarized results of the CYLE-induced current–voltage plot (dark line, mean; gray lines, 95% CL; 6 cells, 5 animals). **D**, Summarized results (black line) showing the change in reversal potential in experiments using different concentrations of extracellular potassium (2.5 mM: -95.5 ± 5.1 mV; 6.5 mM -74.8 ± 3.0 ; 10.5 mM -62.5 ± 4.1 mV; $n=6$, 5 animals). Red dashed line is the calculated Nernst potential in 2.5 K out is -98 mV, -6.5 K out is 72 mV, 10.5 K out is -60 mV). An outwardly rectifying potassium conductance. Supported by Extended Data Figure 2-1. Barium blocks the opioid currents. Supported by Extended Data Figure 2-2. ML297 augments opioid-induced potassium currents. Supported by Extended Data Figure 2-3.

Opioid currents in projection-defined aPVT neurons

The presence of opioid receptors on aPVT neurons with projections to the AM, NAc, or mPFC were examined by responses to ME. Retrograde AAV encoding GFP was microinjected into each area, and recordings were made from GFP-expressing cells (Fig. 4A,B). The currents induced by ME (1 μ M) in recordings from neurons that projected to the AM were larger compared with those projecting to the NAc and mPFC (AM: 72.2 ± 11.0 pA, NAc: 33.5 ± 4.6 pA, mPFC: 39.4 ± 9.2 pA, $n_{AM} = 10$ cells from 5 animals, $n_{NAc} = 10$ cells from 3 animals, $n_{mPFC} = 8$ cells from 3 animals; Fig. 4C). A concentration response to ME indicated that the peak current was reached between 3 and 30 μ M ME (Extended Data Fig. 4-1). The currents measured in projection-defined cells were not different when a saturating concentration of ME (30 μ M) was applied, suggesting that neurons projecting to the AM were more sensitive than those that projected to the NAc or mPFC (Fig. 4D). The capacitance and resting membrane resistance were similar in each projection, indicating that the size and resting conductance of the neurons were not the determinants of the variable amplitude of the opioid current (Fig. 4E,F). Although the sensitivity of neurons varied between neurons with different projections, the extent of desensitization (decline from peak) was similar, indicating that the size of the current was not a determining factor in acute desensitization (Fig. 3D).

Chronic morphine induces tolerance

The effects of chronic opioid treatment were examined following treatment of animals with morphine for 6–7 d using osmotic minipumps (80 mg/kg/d). Receptor-dependent tolerance was investigated using a protocol where slices were prepared and maintained in a concentration of morphine (1 μ M) that approximated the brain concentration induced by the osmotic minipump delivery (Quillinan et al., 2011). Slices from untreated animals were also prepared and maintained

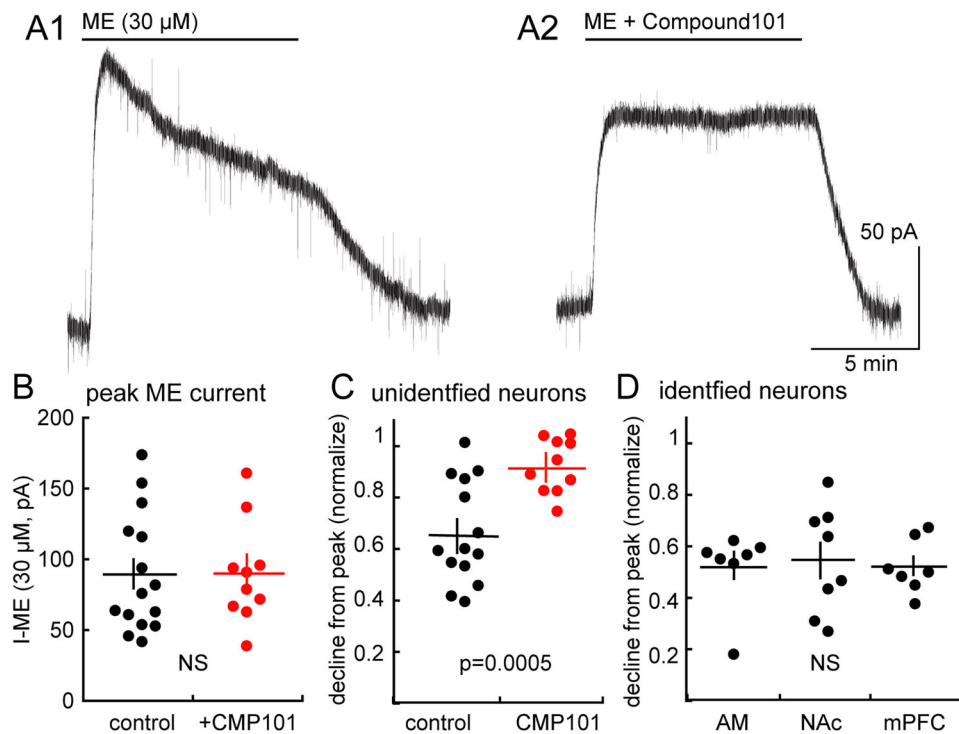


Figure 3. Desensitization of the opioid conductance is phosphorylation dependent. **A**, Example currents induced by ME (30 μM) applied for 10 min in the absence (**A1**) or following incubation with (**A2**) compound 101 (10 μM , 1 h). Note the decline in current (acute desensitization) in **A1** that is abolished following compound 101 treatment (**A2**). **B**, Summarized results showing that the peak current induced by ME (30 μM) was not different in control (88.9 ± 10.8 pA) or compound 101 treated (89.9 ± 11.3 pA) slices (control $n = 15$ cells from 11 animals, CMP101 $n = 10$ cells from 7 animals). **C**, Summarized results of the decline in the ME current in control (black, $65.4 \pm 5.3\%$) and that in slices treated with compound 101 (red, $91.35 \pm 0.03\%$; n as above). **D**, Results obtained with recordings from neurons with projections to the amygdala (AM), nucleus accumbens (NAc), and medial-prefrontal cortex (mPFC).

in the presence of morphine (1 μM). Recordings were made from neurons with identified projections. A steady baseline of 2–5 min in the presence of morphine was obtained prior to the application of naloxone (1 μM). The magnitude of change in holding current induced by naloxone was determined by the difference in the baseline current averaged over 15 s preceding naloxone perfusion and the average current over 15 s measured 5 min following the application of naloxone (Fig. 5). Following the application of naloxone, the peak current (again averaged over a 15 s window centered around the peak) induced by a saturating concentration of baclofen (10 μM) was measured to examine nonspecific alterations the potassium current (Fig. 5). The morphine-dependent current in slices from morphine-treated animals (MTA) was significantly decreased relative to that in slices from untreated controls in AM- and NAc-projecting neurons; there was a trend in mPFC-projecting cells that did not reach statistical significance (AM-Naive: 33.1 ± 5.7 , MTA: 11.7 ± 2.7 , $p = 0.0065$, $n_{\text{Naive}} = 9$ from 4 animals, $n_{\text{MTA}} = 6$ from 4 animals; NAc-Naive: 36.7 ± 3.8 , MTA: 19.2 ± 2.8 , $p = 0.0177$, $n_{\text{Naive}} = 8$ from 4 animals, $n_{\text{MTA}} = 9$ from 4 animals; mPFC-Naive: 34.3 ± 4.0 , MTA: 18.6 ± 3.0 , $p = 0.0714$, $n_{\text{Naive}} = 7$ from 7 animals, $n_{\text{MTA}} = 9$ from 3 animals, 2-way ANOVA with Tukey's test; Fig. 5A,B). The current induced by baclofen was not different in experiments in slices taken from untreated and MTA in any of the three populations (Fig. 5C; $p = 0.2603$, Kruskal–Wallis test) indicating that the tolerance to morphine was specific to morphine (homologous). Only mPFC-projecting aPVT neurons displayed an increase in membrane resistance following chronic morphine treatment (Naive: 248.9 ± 35.1 M Ω , MTA: 365.8 ± 35.1 M Ω , $p = 0.0384$, unpaired t test; Extended Data Fig. 5-1). No difference was seen in the membrane resistance of the other AM- or NAc-projecting neurons (AM: Naive: 295.2 ± 49.7 M Ω ; MTA: 297.2 ± 53.8 M Ω ; $p = 0.5$; NAc: Naive: 249 ± 27.6 M Ω ; MTA: 298.3 ± 50.5 M Ω ; $p = 0.21$, unpaired t tests). Additionally, no change was seen in the capacitance of following chronic morphine treatment (AM: Naive: 18.84 ± 1.39 pF; MTA: 17.9 ± 1.7 pF; $p = 0.67$; NAc: Naive: 19.8 ± 1.3 pF; MTA: 18.2 ± 1.5 pF; $p = 0.44$; mPFC: Naive: 22.6 ± 2.9 pF; MTA: 17.5 ± 1.4 pF; $p = 0.11$, unpaired t tests).

Discussion

This study characterized the acute and chronic actions of opioids on neurons of the anterior paraventricular thalamus (aPVT), highlighting projection-specific differences in both sensitivity and adaptations induced by chronic treatment of animals with morphine. Using a conditional transgenic reporter rat to identify MOR expressing neurons, we observed that most (~90%) aPVT neurons express μ -opioid receptors (MORs). The application of opioids induced an outward current

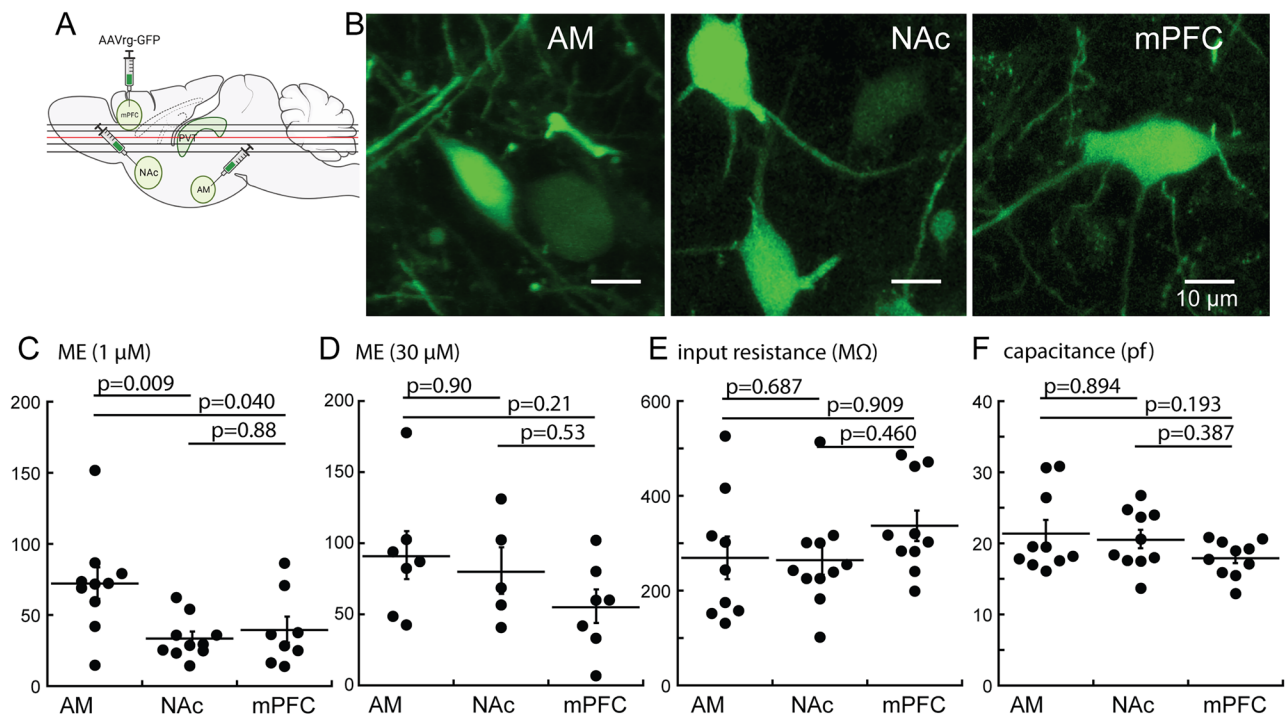


Figure 4. The sensitivity of neurons to ME (1 μM) varied among neurons with different projections. **A**, Schematic illustrating the injection sites of retrograde AAV virus in three projection sites of the aPVT and dorsal/ventral planes where horizontal slices containing the aPVT were collected. **B**, Examples of neurons expressing GFP from each of the projection areas (scale bar 10 μm). **C**, Summary of the current induced by ME (1 μM) in neurons with different projections (AM: 72.2 ± 11.0 pA, NAc: 33.5 ± 4.6 pA, mPFC: 39.4 ± 9.2 pA; held at -70 mV, $n_{\text{AM}} = 10$ from 5 animals, $n_{\text{NAc}} = 10$ from 3 animals, $n_{\text{mPFC}} = 8$ from 3 animals). The current was largest in neurons that projected to the amygdala ($p_{\text{AM vs NAc}} = 0.0088$, $p_{\text{AM vs mPFC}} = 0.0397$, $p_{\text{NAc vs mPFC}} = 0.88$, Tukey's test following one-way ANOVA). **D**, There was no difference in the currents induced by ME (30 μM) in projection neurons (AM: 90.8 ± 16.8 pA, NAc: 79.9 ± 16.3 pA, mPFC: 54.9 ± 11.82 pA, $n_{\text{AM}} = 7$ from 6 animals, $n_{\text{NAc}} = 5$ from 4 animals, $n_{\text{mPFC}} = 7$ from 4 animals; $p > 0.05$, One-way ANOVA). **E**, **F**, The input resistance (**E**; AM: 269.1 ± 45.0 pA, NAc: 264.4 ± 30.9 pA, mPFC: 336.9 ± 32 pA, $n_{\text{AM}} = 10$ from 5 animals, $n_{\text{NAc}} = 11$ from 3 animals, $n_{\text{mPFC}} = 8$ from 3 animals) and capacitance (**F**; AM: 21.4 ± 1.8 pf, NAc: 20.6 ± 1.2 pf, mPFC: 18.5 ± 0.9 pf, $n_{\text{AM}} = 10$ from 5 animals, $n_{\text{NAc}} = 11$ from 3 animals, $n_{\text{mPFC}} = 8$ from 3 animals) of neurons with different projections was not different ($p > 0.05$, one-way ANOVA), suggesting the difference in the current induced by ME was dependent on the coupling of MOR to the potassium conductance. Supported by Extended Data Figure 4-1.

mediated by an increase in potassium conductance that was antagonized by CTAP, a specific MOR antagonist. The outward potassium current was unique in that the current/voltage relationship lacked the typical inward rectification of GIRK channels but was augmented by a positive modulator of GIRK1 channels, ML297. Acute desensitization of the current induced by opioids was dependent on phosphorylation by G-protein receptor kinase 2/3 (GRK2/3), as determined by its blockade by the GRK2/3 inhibitor compound 101. Desensitization as measured by the decline in the peak outward current induced by ME (30 μM , 10 min) measured in the aPVT exhibited an intermediate level ($65 \pm 5\%$) relative to that found in the locus ceruleus where acute desensitization is prominent ($56 \pm 3\%$; Levitt and Williams, 2018) and the Kölliker–Fusé nucleus where desensitization is limited ($72 \pm 14\%$; Levitt and Williams, 2018). Following chronic morphine treatment, a reduction in the current induced by morphine was observed in neurons that project to the AM and NAc. An important limitation of this study is the small sample size and high variance observed within some experimental groups, which could potentially mask underlying differences. Thus, interpretation must be tempered, acknowledging the possibility that larger cohorts or reduced variance might reveal additional meaningful differences. Taken together, however, the results show that the aPVT exhibits both acute responses to MOR activation and adaptive changes following chronic morphine treatment.

Neurons in the PVT contribute to multiple behaviors dependent on the projection target, which can drive distinct aspects of affective or defensive states. For example, the PVT to central AM pathway drives conditioned freezing responses, whereas the PVT to NAc pathway signals active avoidance events (Choi et al., 2010; Oleson et al., 2012; Li et al., 2013; Bravo-Rivera et al., 2014; Penzo et al., 2015; Ramirez et al., 2015; Fadok et al., 2017). In addition, the aPVT and pPVT send nonoverlapping projections to areas including the NAc, amygdala, and mPFC, further highlighting the heterogeneity of the PVT (Gao et al., 2020; Shima et al., 2023). The results from the present study indicate that AM-projecting neurons have a larger potassium-mediated conductance induced by subsaturating ME concentrations when compared with those projecting to the NAc and mPFC. Given that the cell capacitance and input resistance were similar between neurons in each of the projection areas, it is unlikely that cell size and resting conductance play a role in the different amplitudes of the current induced by ME. The response to a saturating concentration of ME was not significantly different between

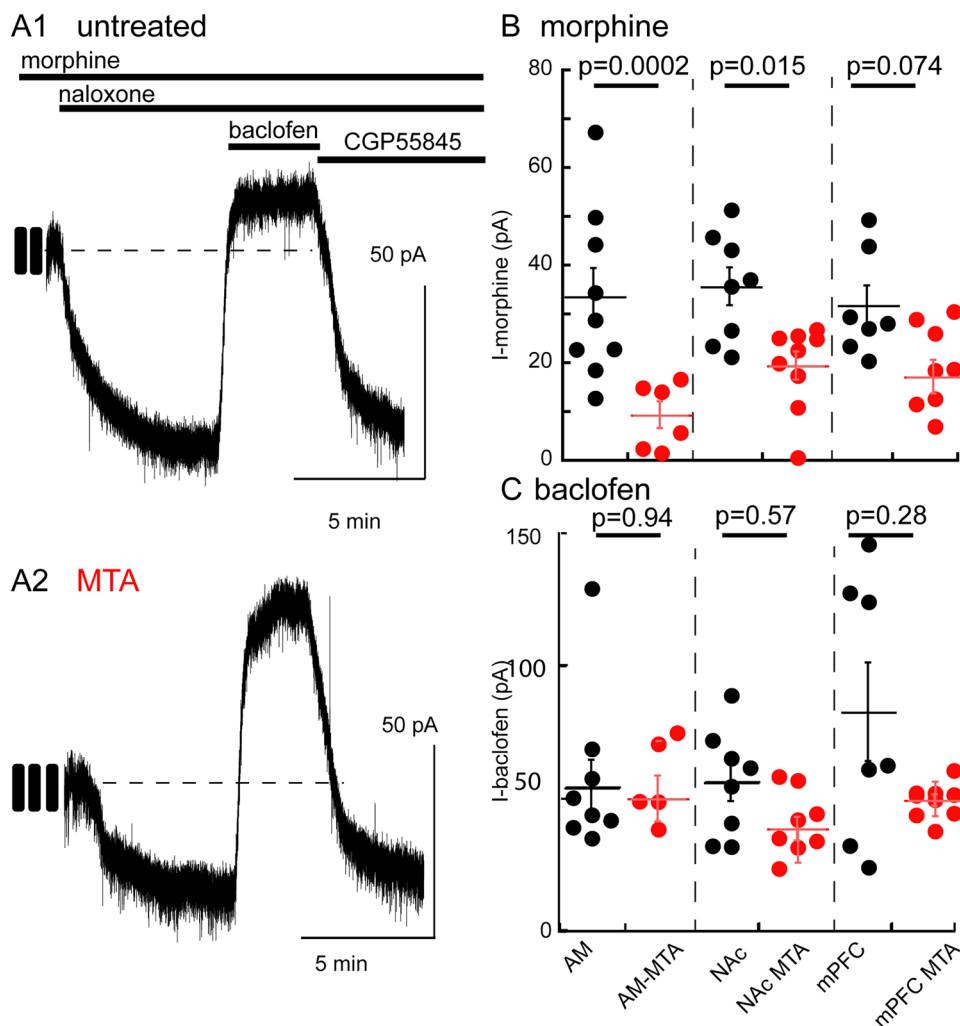


Figure 5. Chronic treatment of animals with morphine-induced tolerance in neurons that projected to the AM and NAc. **A**, Example recordings of the protocol used to determine tolerance to morphine. Slices from untreated (top) and morphine-treated (bottom) animals were cut and maintained in the presence of morphine (1 μ M). Recordings were made and naloxone (1 μ M) was applied to reverse the morphine-induced current. This was followed by the application of baclofen (10 μ M) and CGP55845 (300 nM) to reverse the baclofen-induced current. **B**, Summarized results obtained from untreated (black) and morphine-treated (red) animals. Top, The morphine-dependent current in slices from morphine-treated animals was smaller in neurons projecting to the AM (Naive: 33.1 ± 5.7 , MTA: 11.7 ± 2.7 , $p=0.0065$, Tukey's test following two-way ANOVA, $n_{\text{Naive}}=9$ from 4 animals, $n_{\text{MTA}}=6$ from 4 animals) and NAc (Naive: 36.7 ± 3.8 , MTA: 19.2 ± 2.8 , $p=0.0177$, Tukey's test following two-way ANOVA, $n_{\text{Naive}}=8$ from 4 animals, $n_{\text{MTA}}=9$ from 4 animals) but not those that projected to the mPFC (Naive: 34.3 ± 4.0 , MTA: 18.6 ± 3.0 , $p=0.0714$, Tukey's test following two-way ANOVA, $n_{\text{Naive}}=7$ from 7 animals, $n_{\text{MTA}}=9$ from 3 animals). Bottom, The current induced by baclofen was not different in slices from untreated and morphine-treated animals in all neurons. Supported by Extended Data Figure 5-1.

projections, indicating that AM-projecting neurons are more sensitive to opioids compared with NAc- and mPFC-projecting neurons. Varied coupling of MORs to the potassium conductance or an increased expression of MORs could underlie the difference in current amplitudes at subsaturating concentrations. Functionally, the sensitivity of AM-projecting neurons to opioids may influence emotional processing during opioid use, potentially attenuating affective pain processing. In contrast, the increased receptor-dependent tolerance observed following morphine treatment in neurons projecting to the NAc and mPFC may facilitate motivated behavior toward drug seeking and altered cognitive processes, respectively. Projection-specific adaptations could differentially affect neural circuits within a single brain region involved in opioid use disorder, likely underlying to its multifaceted behavioral manifestations.

The outward current was mediated by a potassium conductance that was distinctive in that the current/voltage (I/V) relationship lacked a typical inward rectification. A previous study indicated that a MOR-mediated hyperpolarization was not solely determined by GIRKs as indicated by the inability of tertipin-Q, a GIRK blocker, to completely block the opioid current or the MOR-mediated hyperpolarization (Hou et al., 2023). The results from that study along with the current/voltage plots of the opioid current made in the present investigation suggest that the underlying conductance is not dependent solely on GIRK channels. Single-cell RNA sequencing revealed expression of the GIRK subunits

KCNJ3, *KCNJ6*, *KCNJ9*, and *KCNJ5* in the aPVT (Gao et al., 2020; Allen Brain Atlas). The fact that ML297 increased the amplitude of the opioid current suggests that GIRK1 may be involved; however, ML297 did not induce an increase in inward rectification or alter the shape of the current/voltage plot. This suggests a complex interaction between GIRK channels and likely other potassium channels affecting neuronal excitability. The identity of the potassium conductance activated by opioids remains a question. One possibility is the two-pore domain potassium (K2P) channel family. Knockout mice lacking TREK-1 channels were significantly less sensitive to morphine, indicating that opioids could act through this channel (Devilliers et al., 2013). In addition, morphine caused an outward current in COS cells expressing TREK-1 channels, and the current–voltage plot was similar to that found in the present study (Devilliers et al., 2013). Thus, the conductance underlying the outward current in the PVT may involve K2P channels, potentially in conjunction with GIRK channels, reflecting a complex interplay that affects neuronal excitability.

Projections to the NAc, mPFC, and AM are likely all key areas in both the positive and negative aspects of acute and chronic actions of opioids. The symptoms of acute withdrawal are thought to contribute to opioid use disorder in that continued drug seeking is maintained to avoid aversive states (Koob and Volkow, 2016; Koob, 2020). The connections between the PVT and limbic structures, such as the amygdala and NAc, play critical roles in processing such negative states. Naloxone-induced withdrawal results in a substantial increase in *c-fos* expression in the PVT as well as potentiated signaling from PVT cells on to D_2 receptor expressing cells in the NAc (Zhu et al., 2016). The role of pre- and postsynaptic adaptations in altered PVT activity have yet to be fully explored; however, it is likely that both contribute to such effects. The concept of hyperkatifeia, or increased sensitivity to emotional distress, is one well-studied aspect of the motivational aspects of continued opioid use (Koob, 2020). The aPVT is poised to encode this increased sensitivity through its influence on limbic circuits, reinforcing drug-seeking behavior as a means to alleviate negative emotional states following chronic drug use.

References

- Avidsson U, Riedl M, Chakrabarti S, Lee JH, Nakano AH, Dado RJ, Loh HH, Law PY, Wessendorf MW, Elde R (1995) Distribution and targeting of a mu-opioid receptor (MOR1) in brain and spinal cord. *J Neurosci* 15:3328–3341.
- Babaei F, Kourosh-Arami M, Farhadi M (2023) NMDA receptors in the rat paraventricular thalamic nucleus reduce the naloxone-induced morphine withdrawal. *Cent Nerv Syst Agents Med Chem* 23:119–125.
- Banghart MR, Sabatini BL (2012) Photoactivatable neuropeptides for spatiotemporally precise delivery of opioids in neural tissue. *Neuron* 73:249–259.
- Barson JR, Mack NR, Gao W-J (2020) The paraventricular nucleus of the thalamus is an important node in the emotional processing network. *Front Behav Neurosci* 14:598469.
- Bengoetxea X, Goedecke L, Blaesse P, Pape H-C, Jüngling K (2020) The μ -opioid system in midline thalamic nuclei modulates defence strategies towards a conditioned fear stimulus in male mice. *J Psychopharmacol Oxf Engl* 34:1280–1288.
- Birdsong WT, Williams JT (2020) Recent advances in understanding neuronal adaptations to opioid drugs. *Mol Pharmacol* 98:542–551.
- Bossert JM, et al. (2023) Effect of selective lesions of nucleus accumbens μ -opioid receptor-expressing cells on heroin self-administration in male and female rats: a study with novel Oprm1-Cre knock-in rats. *J Neurosci* 43:1692–1713.
- Bravo-Rivera C, Roman-Ortiz C, Brignoni-Perez E, Sotres-Bayon F, Quirk GJ (2014) Neural structures mediating expression and extinction of platform-mediated avoidance. *J Neurosci* 34:9736–9742.
- Bu X, Chen Y, Lv P, Fu X, Fu B (2022) Glutamatergic neurons in paraventricular nucleus of the thalamus regulate the recovery from isoflurane anesthesia. *BMC Anesthesiol* 22:256.
- Chahl LA, Leah J, Herdegen T, Trueman L, Lynch-Frame AM (1996) Distribution of c-Fos in guinea-pig brain following morphine withdrawal. *Brain Res* 717:127–134.
- Chang Y-T, Chen W-H, Shih H-C, Min M-Y, Shyu B-C, Chen C-C (2019) Anterior nucleus of paraventricular thalamus mediates chronic mechanical hyperalgesia. *Pain* 160:1208.
- Chisholm A, Iannuzzi J, Rizzo D, Gonzalez N, Fortin É, Bumbu A, Batallán Burrowes AA, Chapman CA, Shalev U (2020) The role of the paraventricular nucleus of the thalamus in the augmentation of heroin seeking induced by chronic food restriction. *Addict Biol* 25:e12708.
- Choi J-S, Cain CK, LeDoux JE (2010) The role of amygdala nuclei in the expression of auditory signaled two-way active avoidance in rats. *Learn Mem Cold Spring Harb N* 17:139–147.
- Devilliers M, et al. (2013) Activation of TREK-1 by morphine results in analgesia without adverse side effects. *Nature Com* 4:2941.
- Dong X, Li S, Kirouac GJ (2020) A projection from the paraventricular nucleus of the thalamus to the shell of the nucleus accumbens contributes to footshock stress-induced social avoidance. *Neurobiol Stress* 13:100266.
- Duan W-Y, Peng K, Qin H-M, Li B-M, Xu Y-X, Wang D-J, Yu L, Wang H, Hu J, Wang Q-X (2024) Esketamine accelerates emergence from isoflurane general anaesthesia by activating the paraventricular thalamus glutamatergic neurons in mice. *Br J Anaesth* 132:334–342.
- Eacret D, Manduchi E, Noreck J, Tyner E, Fenik P, Dunn AD, Schug J, Veasey SC, Blendy JA (2023) Mu-opioid receptor-expressing neurons in the paraventricular thalamus modulate chronic morphine-induced wake alterations. *Transl Psychiatry* 13:78.
- Fadok JP, et al. (2017) A competitive inhibitory circuit for selection of active and passive fear responses. *Nature* 542:96–100.
- Gao C, Leng Y, Ma J, Rooke V, Rodriguez-Gonzalez S, Ramakrishnan C, Deisseroth K, Penzo MA (2020) Two genetically, anatomically and functionally distinct cell types segregate across anteroposterior axis of paraventricular thalamus. *Nat Neurosci* 23:217–228.
- Giannotti G, Gong S, Fayette N, Heinsbroek JA, Orfila JE, Herson PS, Ford CP, Peters J (2021) Extinction blunts paraventricular thalamic contributions to heroin relapse. *Cell Rep* 36:109605.
- Hou G, Jiang S, Chen G, Deng X, Li F, Xu H, Chen B, Zhu Y (2023) Opioid receptors modulate firing and synaptic transmission in the paraventricular nucleus of the thalamus. *J Neurosci* 43:2682–2695.
- Huong H, Ghosh P, van den Pol AN (2006) Prefrontal cortex–projecting glutamatergic thalamic paraventricular nucleus–excited by hypocretin: a feedforward circuit that may enhance cognitive arousal. *J Neurophysiol* 95:1656–1668.
- Igarashi H, Koizumi K, Kaneko R, Ikeda K, Egawa R, Yanagawa Y, Muramatsu S, Onimaru H, Ishizuka T, Yawo H (2016) A novel reporter rat strain that conditionally expresses the bright red fluorescent protein tdTomato. *PLoS One* 11:e0155687.

- Kanai M, Kamiizawa R, Hitora-Imamura N, Minami M (2022) Exposure to hot and cold environments activates neurons projecting from the paraventricular thalamic nucleus to brain regions related to approach and avoidance behaviors. *J Therm Biol* 103:103157.
- Keyes PC, Adams EL, Chen Z, Bi L, Nachtrab G, Wang VJ, Tessier-Lavigne M, Zhu Y, Chen X (2020) Orchestrating opiate-associated memories in thalamic circuits. *Neuron* 107:1113–1123.e4.
- Kirouac GJ (2015) Placing the paraventricular nucleus of the thalamus within the brain circuits that control behavior. *Neurosci Biobehav Rev* 56:315–329.
- Kolaj M, Zhang L, Rönnekleiv OK, Renaud LP (2012) Midline thalamic paraventricular nucleus neurons display diurnal variation in resting membrane potentials, conductances, and firing patterns in vitro. *J Neurophysiol* 107:1835–1844.
- Kolaj M, Zhang L, Hermes MLHJ, Renaud LP (2014) Intrinsic properties and neuropharmacology of midline paraventricular thalamic nucleus neurons. *Front Behav Neurosci* 8:132.
- Koob GF (2013) Addiction is a reward deficit and stress surfeit disorder. *Front Psychiatry* 4:72.
- Koob GF (2020) Neurobiology of opioid addiction: opponent process, hyperkatifeia, and negative reinforcement. *Biol Psychiatry* 87:44–53.
- Koob GF, Volkow ND (2016) Neurobiology of addiction: a neurocircuitry analysis. *Lancet Psychiatry* 3:760–773.
- Leff ER, Arttamangkul S, Williams JT (2020) Chronic treatment with morphine disrupts acute kinase-dependent desensitization of GPCRs. *Mol Pharmacol* 98:497–507.
- Le Merrer J, Becker JA, Befort K, Kieffer BL (2009) Reward processing by the opioid system in the brain. *Physiol Rev* 89:1379–1412.
- Levitt ES, Williams JT (2018) Desensitization and tolerance of Mu opioid receptors on pontine Kölliker-Fuse neurons. *Mol Pharmacol* 93:8–13.
- Li H, Penzo MA, Taniguchi H, Kopec CD, Huang ZJ, Li B (2013) Experience-dependent modification of a central amygdala fear circuit. *Nat Neurosci* 16:332–339.
- Li S, Kirouac GJ (2008) Projections from the paraventricular nucleus of the thalamus to the forebrain, with special emphasis on the extended amygdala. *J Comp Neurol* 506:263–287.
- Li S, Kirouac GJ (2012) Sources of inputs to the anterior and posterior aspects of the paraventricular nucleus of the thalamus. *Brain Struct Funct* 217:257–273.
- Lowe JD, et al. (2015) Role of G protein-coupled receptor kinases 2 and 3 in μ -opioid receptor desensitization and internalization. *Mol Pharm* 88:347–356.
- Lüscher C, Slesinger PA (2010) Emerging roles for G protein-gated inwardly rectifying potassium (GIRK) channels in health and disease. *Nat Rev Neurosci* 11:301–315.
- Ma J, du Hoffmann J, Kindel M, Sofia Beas B, Chudasama Y, Penzo MA (2021) Divergent projections of the paraventricular nucleus of the thalamus mediate the selection of passive and active defensive behaviors. *Nat Neurosci* 24:1429–1440.
- Mansour A, Fox CA, Akil H, Watson SJ (1994) Opioid-receptor mRNA expression in the rat CNS: anatomical and functional implications. *Trends Neurosci* 17:22–29.
- McDevitt DS, Wade QW, McKendrick GE, Nelsen J, Starostina M, Tran N, Blendy JA, Graziane NM (2024) The paraventricular thalamic nucleus and its projections in regulating reward and context associations. *eNeuro* 11:ENEURO.0524-23.2024.
- McDevitt DS, Graziane NM (2019) Timing of morphine administration differentially alters paraventricular thalamic neuron activity. *eNeuro* 6:1–14.
- Oleson EB, Gentry RN, Chioma VC, Cheer JF (2012) Subsecond dopamine release in the nucleus accumbens predicts conditioned punishment and its successful avoidance. *J Neurosci* 32:14804–14808.
- O'Neill P-K, Posani L, Meszaros J, Warren P, Schoonover CE, Fink AJP, Fusi S, Salzman CD (2023) The representational geometry of emotional states in basolateral amygdala. *BioRxiv Prepr. Serv. Biol.* 2023.09.23.558668.
- Otis JM, et al. (2019) Paraventricular thalamus projection neurons integrate cortical and hypothalamic signals for Cue-reward processing. *Neuron* 103:423–431.e4.
- Padilla-Coreano N, Do-Monte FH, Quirk GJ (2012) A time-dependent role of midline thalamic nuclei in the retrieval of fear memory. *Neuropharmacology* 62:457–463.
- Paniccia JE, et al. (2024) Restoration of a paraventricular thalamo-accumbal behavioral suppression circuit prevents reinstatement of heroin seeking. *Neuron* 112:772–785.e9.
- Penzo MA, et al. (2015) The paraventricular thalamus controls a central amygdala fear circuit. *Nature* 519:455–459.
- Penzo MA, Gao C (2021) The paraventricular nucleus of the thalamus: an integrative node underlying homeostatic behavior. *Trends Neurosci* 44:538–549.
- Piantadosi SC, Zhou ZC, Pizzano C, Pedersen CE, Nguyen TK, Thai S, Stuber GD, Bruchas MR (2024) Holographic stimulation of opposing amygdala ensembles bidirectionally modulates valence-specific behavior via mutual inhibition. *Neuron* 112:593–610.e5.
- Pickens CL, Airavaara M, Theberge F, Fanous S, Hope BT, Shaham Y (2011) Neurobiology of the incubation of drug craving. *Trends Neurosci* 34:411–420.
- Pologruto TA, Sabatini BL, Svoboda K (2003) Scanimage: flexible software for operating laser scanning microscopes. *BioMed Eng OnLine* 2:13.
- Quillinan N, Lau EK, Virk M, von Zastrow M, Williams JT (2011) Recovery from μ -opioid receptor desensitization after chronic treatment with morphine and methadone. *J Neurosci* 31:4434–4443.
- Ramirez F, Moscarello JM, LeDoux JE, Sears RM (2015) Active avoidance requires a serial basal amygdala to nucleus accumbens shell circuit. *J Neurosci* 35:3470–3477.
- Rivera-Irizarry JK, Hámor PU, Rowson SA, Asfour J, Liu D, Zallar LJ, Garcia AF, Skelly MJ, Plei KE (2023) Valence and salience encoding by parallel circuits from the paraventricular thalamus to the nucleus accumbens. *BioRxiv Prepr. Serv. Biol.* 2023.07.03.547570.
- Shima Y, et al. (2023) Distinctiveness and continuity in transcriptome and connectivity in the anterior-posterior axis of the paraventricular nucleus of the thalamus. *Cell Rep* 42:113309.
- Tang Q-Q, Wu Y, Tao Q, Shen Y, An X, Liu D, Xu Z (2024) Direct paraventricular thalamus-basolateral amygdala circuit modulates neuropathic pain and emotional anxiety. *Neuropsychopharmacol* 49:455–466.
- Williams JT, Ingram SL, Henderson G, Chavkin C, von Zastrow M, Schulz S, Koch T, Evans CJ, Christie MJ (2013) Regulation of μ -opioid receptors: desensitization, phosphorylation, internalization, and tolerance. *Pharmacol Rev* 65:223–254.
- Wydeven N, Marron Fernandez de Velasco E, Du Y, Benneyworth MA, Hearing MC, Fischer RA, Thomas MJ, Weaver CD, Wickman K (2014) Mechanisms underlying the activation of G-protein-gated inwardly rectifying K⁺ (GIRK) channels by the novel anxiolytic drug, ML297. *Proc Natl Acad Sci U S A* 111:10755–10760.
- Yu L, Chu C, Yuan Y, Guo X, Lei C, Sheng H, Yang L, Cui D, Lai B, Zheng P (2021) Activity in projection neurons from prelimbic cortex to the PVT is necessary for retrieval of morphine withdrawal memory. *Cell Rep* 35:108958.
- Zhang G, et al. (2023) Neural and molecular investigation into the paraventricular thalamic-nucleus accumbens circuit for pain sensation and non-opioid analgesia. *Pharmacol Res* 191:106776.
- Zhang W-T, Sha W-L, Zhu Q, Wu X-B, He C (2022) Plasticity of neuronal excitability and synaptic balance in the anterior nucleus of paraventricular thalamus after nerve injury. *Brain Res Bull* 188:1–10.
- Zhao J, et al. (2022) A paraventricular thalamus to central amygdala neural circuit modulates acute stress-induced heightened wakefulness. *Cell Rep* 41:111824.
- Zhu Y, Wienecke CFR, Nachtrab G, Chen X (2016) A thalamic input to the nucleus accumbens mediates opiate dependence. *Nature* 530:219–222.
- Zhu Y, et al. (2023) Nucleus accumbens D1/D2 circuits control opioid withdrawal symptoms in mice. *J Clin Invest* 133:e163266.